

LRP 659/00

January 2000

**Power laws for the spatial dependence of
electrical parameters in the high voltage,
capacitive RF sheath**

H. Müller, A.A. Howling, Ch. Hollenstein

submitted for publication in
IEEE Transactions on Plasma Science

Power Laws for the Spatial Dependence of Electrical Parameters in the High Voltage, Capacitive rf Sheath

H. Müller, A.A. Howling, Ch. Hollenstein

Centre de Recherches en Physique des Plasmas, Ecole Polytechnique Fédérale de Lausanne,
PPB-Ecublens, CH-1015 Lausanne, Switzerland

Abstract

Following the analytical description of the collisionless, high voltage, capacitive rf sheath in M. A. Lieberman, IEEE Trans. Plasma Sci. **16**, 638 (1988), and of the collisional, high voltage, capacitive rf sheath in M. A. Lieberman, IEEE Trans. Plasma Sci. **17**, 338 (1989), electrical sheath parameters for a square wave rf discharge current are calculated. The interest in the square wave current lies in the analytical simplicity of the solutions. The results are compared with Lieberman's results for the sinusoidal rf discharge current. The spatial dependences of the time-averaged electric potential, electric field, net charge carrier density, and of the ion density, turn out to be very similar for the two current wave-forms. The rf sheath analysis for the square wave current reveals that these parameters are related to the distance from the plasma / sheath edge by power laws.

For the collisionless rf sheath, the respective exponents are $3/2$, $1/2$, $-1/2$, and $-3/4$ (compared to $4/3$, $1/3$, $-2/3$, $-2/3$ for the collisionless dc sheath).

For the collisional rf sheath, the respective exponents are 2 , 1 , 0 , and $-1/2$ (compared to $5/3$, $2/3$, $-1/3$, $-1/3$ for the collisional dc sheath).

Parameter	Symbol (SI & normalized)	
electron temperature (Volt)	T_e	
electron density	n_e	
ion mass	m_i	
ion velocity	v_i	
discharge fundamental angular frequency	ω	
distance plasma / sheath edge to electrode = sheath width	d	
ion current per unit area	J_i	
total current per unit area	J_t	
time, phase angle	t	φ
sheath charge per unit area	q	$1 - r$
distance from the plasma / sheath edge	x	ξ
distance plasma / sheath edge to electron step	s	σ
ion density	n_i	v_i
time-averaged net charge carrier density	$\bar{n} = n_i - \bar{n}_e$	v
time-averaged electric field	\bar{E}	ε
time-averaged potential	$\bar{\Phi}$	η
sheath voltage	U	u

The normalization of the rf sheath parameters is defined in section IV. Throughout this report, current per unit area and charge per unit area are referred to as current and charge, and the time-averaged potential, time-averaged electric field, and time-averaged net charge carrier density are referred to as potential, electric field, and net charge carrier density.

I. Introduction

Capacitive rf gas discharges are widely used for material surface processing (sputtering, etching, film deposition) eg in the semiconductor industry. Gas discharge models, ie models for the bulk plasma and for the sheaths between the bulk plasma and the electrodes, are therefore of practical interest.

Lieberman devised a model for the high voltage, capacitive rf sheath allowing analytical solution. For the input parameters, amplitude of the sinusoidal discharge current (rf), and ion current (constant), he calculated space or time dependences of electrical sheath parameters, and the sheath width and voltage, both for collisionless [1] and for (highly) collisional [2] ion motion through the sheath. The time-dependence of the discharge current, ie the current waveform, was chosen sinusoidal, according to industrial plasma practice. In this report Lieberman's rf sheath analysis is carried out for a square wave discharge current. This current waveform is not commonly used, but leads to simple analytical solutions for all sheath parameters, allowing new insights into the electrical properties of the rf sheath.

In section II we present the assumptions of the rf sheath model.

In section III, we list the equations determining the space-time behaviour of the rf sheath.

In section IV, we normalize the sheath parameters and equations.

In section V, we calculate the general rf sheath solution.

In section VI, we calculate the rf sheath solution for the square wave discharge current.

In section VII, we compare the rf sheath solutions for square wave discharge current, derived in this report, and for sinusoidal discharge current, calculated by Lieberman in refs. [1, 2].

The results are discussed in section VIII.

II. Model of the High Voltage, Capacitive rf Sheath

The terms "capacitive rf sheath" (ie, the angular frequency of the discharge current lies between the plasma angular frequencies of the ions and of the electrons : $\omega_{pi} < \omega < \omega_{pe}$) and "high voltage rf sheath" (ie, the electron temperature is much smaller than the time-averaged sheath voltage : $T_e \ll \bar{U}$) indicate the simplifying assumptions of the sheath model.

Capacitive rf sheath :

- A1 The ions respond to the time-averaged electric field.
- A2 The electrons have no inertia, ie they respond immediately to the electric field.

High voltage rf sheath :

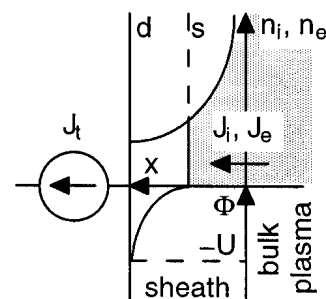
- A3 The Debye length is much shorter than the sheath width : $\lambda_D \ll d$. The electron density in the sheath is discontinuous : $n_e = n_i$ for $x < s$, $n_e = 0$ for $x > s$, see fig. 1.
- A4 The electric field at the plasma / sheath edge is negligible : $\bar{E}(x = 0) = 0$.
- A5 The ions enter the sheath with negligible velocity : $v_i(x = 0) = 0$.

Furthermore we assume :

- A6 Ionization in the sheath is negligible.
- A7 Secondary electron emission from the electrode, due to ion impact, is negligible.

figure 1:

Schematic representation of the high voltage, capacitive rf sheath model.



The sheath model is shown schematically in fig. 1. The discharge current = total current J_t is positiv when flowing to the left. The electron step then moves to the right. The ion density diverges at the plasma / sheath edge : we assume a finite ion current $J_i = en_i v_i$ entering the sheath with velocity $v_i = 0$ (A5). The total current J_t is the sum of ion current, electron current and displacement current. J_t is conserved for any discharge cross section. The ion current J_i is conserved in the sheath (A1, A6, A7). The sum of electron current and displacement current, $J_t - J_i$, is also conserved in the sheath. $J_t - J_i$ is purely electron current for $0 < x < s$, and purely displacement current for $s < x < d$ (A3).

III. rf Sheath Equations

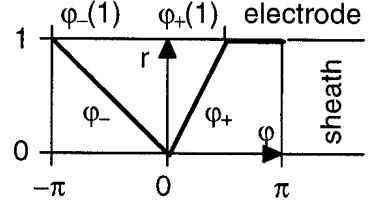
The analytical description of the collisionless rf sheath in [1] and of the collisional rf sheath in [2] is now reproduced. We consider the total rf current $J_t(t)$ and the ion current J_i as the input parameters. We *drop* Lieberman's assumption of small ion current ($J_i \ll J_t$), and introduce a new variable r , the ratio, number of electrons N_e to number of ions N_i in the sheath :

$$r = \frac{N_e}{N_i} \quad (1)$$

By definition, $0 \leq r \leq 1$. For $r = 0$, the electron step is at the plasma / sheath edge : $s = 0$; for $r = 1$, the electron step is at the electrode : $s = d$. The relation between r and the rf phase angle $\varphi = \omega t$ is shown in fig. 2. We assume that the sheath charges up ($J_t - J_i > 0$) for $\varphi_-(r = 1) < \varphi < 0$, and discharges ($J_t - J_i < 0$) for $0 < \varphi < \varphi_+(r = 1)$. To each value of r correspond a positive and a negative phase angle φ_+ and φ_- .

figure 2 :

Electron to ion ratio in the sheath $r = N_e / N_i$, versus rf phase angle $\varphi = \omega t$, shown for a square wave total current. Due to the ion current, the sheath discharges more rapidly than it charges up, and the electron step connects with the electrode before the end of the rf period.



We relate the sheath charge q to the current $J_t - J_i$:

$$dq = \begin{cases} 0 & -\pi < \varphi < \varphi_-(1) \\ d\varphi \frac{J_t - J_i}{\omega} & \varphi_-(1) < \varphi < \varphi_+(1) \\ 0 & \varphi_+(1) < \varphi < \pi \end{cases} \quad (2)$$

Using (2), we determine the sheath charge amplitude \tilde{q} :

$$\tilde{q} = e \times \frac{N_i}{2} = \begin{cases} \frac{1}{2} \int_{-\pi}^0 d\varphi \frac{dq}{d\varphi} = \int_{\varphi_-(1)}^0 d\varphi \frac{J_t - J_i}{2\omega} & (3.1) \\ -\frac{1}{2} \int_0^{\pi} d\varphi \frac{dq}{d\varphi} = -\int_0^{\varphi_+(1)} d\varphi \frac{J_t - J_i}{2\omega} & (3.2) \end{cases}$$

Using (2), we determine the time-averaged sheath charge \bar{q} :

$$\bar{q} = \frac{1}{2\pi} \int_{-\pi}^{\pi} d\varphi q = -\int_{-\pi}^{\pi} d\varphi \frac{dq}{d\varphi} \frac{\varphi}{2\pi} = -\int_{\varphi_-(1)}^{\varphi_+(1)} d\varphi \frac{J_t - J_i}{\omega} \frac{\varphi}{2\pi} \quad (4)$$

\tilde{q} and \bar{q} are useful parameters for normalization, section IV.

Using (1), we relate the sheath charge q to the new sheath variable r :

$$dq = -edN_e = -eN_1 dr = -2\tilde{q} dr \quad (5)$$

Combining (2) and (5), we obtain an equation for the phase angles $\varphi_+(r)$ and $\varphi_-(r)$:

$$r = \begin{cases} \int_{\varphi^-}^0 d\varphi \frac{J_t - J_i}{2\tilde{q}\omega} & (6.1) \\ -\int_0^{\varphi^+} d\varphi \frac{J_t - J_i}{2\tilde{q}\omega} & (6.2) \end{cases}$$

From (A3) follows a relation between the sheath charge q and the distance plasma / sheath edge to electron step, s :

$$dq = -en_i ds \quad (7)$$

Combining (5) and (7), we obtain an equation for $s(r)$:

$$\frac{ds}{dr} = 2 \frac{\tilde{q}}{en_i} \quad (8)$$

r can act as a time-coordinate by its relation to the rf phase angle, (6), and as a spatial coordinate by its relation to the electron step position, (8). Whenever a space-dependent quantity (eg n_i in (8)) appears in an equation together with r , or $\varphi_+(r)$, $\varphi_-(r)$, it must be evaluated at $x = s(r)$.

The ratio, net charge carrier density to ion density, is equal to the fraction of time per rf cycle when the ions are not screened by the electrons :

$$\frac{\bar{n}}{n_i} = \frac{\varphi_+ - \varphi_-}{2\pi} \quad (9)$$

We reformulate Maxwell's source equation for the electric field, using (8) :

$$\frac{d\bar{E}}{dx} = \frac{e}{\epsilon_0} \bar{n} \quad \xrightarrow{x=r} \quad \frac{d\bar{E}}{dr} = 2 \frac{\tilde{q}}{\epsilon_0} \frac{\bar{n}}{n_i} \quad (10)$$

We reformulate the definition of the electrostatic potential, using (8) :

$$-\frac{d\bar{\Phi}}{dx} = \bar{E} \quad \xrightarrow{x=r} \quad -\frac{d\bar{\Phi}}{dr} = 2 \frac{\tilde{q}}{e} \frac{\bar{E}}{n_i} \quad (11)$$

Collisionless ion motion is determined by ion energy conservation :

$$\frac{m_i}{e} \frac{v_i^2}{2} = -\bar{\Phi} \quad (12a)$$

From the ion mobility law for fast, collisional ion motion [3a] follows :

$$\frac{m_i}{e} \frac{v_i^2}{\frac{2}{\pi} \lambda_i} = \bar{E} \quad (12b)$$

The (conserved) ion current is

$$J_i = en_i v_i \quad (13)$$

To eliminate the ion velocity, we insert **(12)** into **(13)** :

$$J_i = en_i \sqrt{\frac{-2e\bar{\Phi}}{m_i}} \quad (14a)$$

$$J_i = en_i \sqrt{\frac{2}{\pi} \lambda_1 \frac{e\bar{E}}{m_i}} \quad (14b)$$

The sheath voltage $U(t)$ can be related to $s(t)$ and $n_i(x)$ by integrating Poisson's equation :

$$U = \int_s^d dx \int_s^x dx' \frac{en_i(x')}{\epsilon_0} \quad (15)$$

By time-differentiating **(15)**, and applying the mathematical identity

$$\frac{d}{dt} \int_{a(t)}^{b(t)} dx f(x,t) = f(b(t),t) \frac{db}{dt} - f(a(t),t) \frac{da}{dt} + \int_{a(t)}^{b(t)} dx \frac{\partial}{\partial t} f(x,t)$$

we obtain, after some calculation, a more convenient equation for $U(t)$:

$$\frac{dU}{dt} = -(d-s) \frac{ds}{dt} \frac{e}{\epsilon_0} n_i(s) \quad \rightarrow \quad dU = -2\tilde{q} dr \times \frac{d-s}{\epsilon_0} \quad (16)$$

In the last step we have again used **(8)**.

(16) is formally analogous to the capacitance equation $dU = dq/C$. An increase of sheath voltage is due to ion charge uncovered by the moving electron step.

IV. Normalization

The procedure to obtain the rf sheath solution is to calculate, for a specific total current $J_t(\varphi)$, $\varphi_+(r)$ and $\varphi_-(r)$ from (6). Equations (8) – (11), (14), (16) can then be solved for $n_i(r)$, $\bar{n}(r)$, $\bar{E}(r)$, $\bar{\Phi}(r)$, $s(r)$, $U(r)$. To facilitate the task, it is useful to normalize these sheath parameters. The normalization is presented as 'normalized parameter' \times 'unit' = 'parameter'.

$$\varepsilon \times \frac{\bar{q}}{\varepsilon_0} = \bar{E} \quad (17)$$

Collisionless rf sheath

$$\left. \begin{array}{l} \xi \\ \sigma \end{array} \right\} \times \frac{\tilde{q}^2}{J_i^2} \frac{e\bar{q}}{\varepsilon_0 m_i} = \left\{ \begin{array}{l} x \\ s \end{array} \right. \quad (18a)$$

$$\left. \begin{array}{l} v \\ v_i \frac{\tilde{q}}{\bar{q}} \end{array} \right\} \times \frac{J_i^2}{\tilde{q}^2} \frac{\varepsilon_0 m_i}{e^2} = \left\{ \begin{array}{l} \bar{n} \\ n_i \end{array} \right. \quad (20a)$$

$$\left. \begin{array}{l} \eta \\ u \frac{\tilde{q}}{\bar{q}} \end{array} \right\} \times \frac{\tilde{q}^2}{J_i^2} \frac{e\bar{q}^2}{\varepsilon_0^2 m_i} = \left\{ \begin{array}{l} -\bar{\Phi} \\ U \end{array} \right. \quad (22a)$$

$$\left. \begin{array}{l} \eta \\ u \frac{\tilde{q}}{\bar{q}} \end{array} \right\} \times \frac{\tilde{q}^2}{J_i^2} \frac{e\bar{q}^2}{\varepsilon_0^2 m_i} = \left\{ \begin{array}{l} U \end{array} \right. \quad (23a)$$

Collisional rf sheath

$$\left. \begin{array}{l} \xi \\ \sigma \end{array} \right\} \times \frac{\tilde{q}}{J_i} \left(\frac{\frac{2}{\pi} \lambda_i \bar{q} e}{\varepsilon_0 m_i} \right)^{1/2} = \left\{ \begin{array}{l} x \\ s \end{array} \right. \quad (18b)$$

$$\left. \begin{array}{l} v \\ v_i \frac{\tilde{q}}{\bar{q}} \end{array} \right\} \times \frac{J_i}{\tilde{q}} \frac{\varepsilon_0}{e} \left(\frac{\bar{q} m_i}{\varepsilon_0 e \frac{2}{\pi} \lambda_i} \right)^{1/2} = \left\{ \begin{array}{l} \bar{n} \\ n_i \end{array} \right. \quad (20b)$$

$$\left. \begin{array}{l} \eta \\ u \frac{\tilde{q}}{\bar{q}} \end{array} \right\} \times \frac{\tilde{q}}{J_i} \left(\frac{e\bar{q}^3 \frac{2}{\pi} \lambda_i}{\varepsilon_0^3 m_i} \right)^{1/2} = \left\{ \begin{array}{l} -\bar{\Phi} \\ U \end{array} \right. \quad (22b)$$

$$\left. \begin{array}{l} \eta \\ u \frac{\tilde{q}}{\bar{q}} \end{array} \right\} \times \frac{\tilde{q}}{J_i} \left(\frac{e\bar{q}^3 \frac{2}{\pi} \lambda_i}{\varepsilon_0^3 m_i} \right)^{1/2} = \left\{ \begin{array}{l} U \end{array} \right. \quad (23b)$$

We note that from (3), (4) follows in the limit of small ion current, $J_i/J_t \rightarrow 0$:

$$\tilde{q} = \bar{q} = \tilde{J}_t / \omega \text{ for the sinusoidal total current } J_t = -\tilde{J}_t \sin \varphi, \text{ and}$$

$$\tilde{q} = \bar{q} = \frac{\pi}{2} |J_t| / \omega \text{ for the square wave total current } J_t = -|J_t| \text{sign}(\varphi) \text{ (with } |J_t| \text{ a constant).}$$

Our normalization of the sheath parameters is almost identical to Lieberman's normalization in [1,2]; the conversion is explained in the Appendix.

From the normalization of s , (19), and of $\bar{\Phi}$, (22) follows the general form of the Child law for the rf sheath. We abbreviate $r = 0$ and $r = 1$ by indices 0 and 1.

(24a) is obtained by calculating $(-\bar{\Phi}_1)^{3/2}/s_1^2 = \bar{U}^{3/2}/d^2$.

(24b) is obtained by calculating $(-\bar{\Phi}_1)^{3/2}/s_1^{5/2} = \bar{U}^{3/2}/d^{5/2}$.

Collisionless rf sheath

Collisional rf sheath

$$J_i = K \epsilon_0 \sqrt{\frac{2e}{m_i} \frac{\bar{U}^{3/2}}{d^2}} \quad (24.1a)$$

$$J_i = K \epsilon_0 \sqrt{\frac{2e}{m_i} \frac{2}{\pi} \lambda_i \frac{\bar{U}^{3/2}}{d^{5/2}}} \quad (24.1b)$$

where

where

$$K = \frac{\tilde{q}}{\bar{q}} \sqrt{\frac{1}{2} \frac{\sigma_1^4}{\eta_1^3}} \quad (24.2a)$$

$$K = \frac{\tilde{q}}{\bar{q}} \sqrt{\frac{1}{2} \frac{\sigma_1^5}{\eta_1^3}} \quad (24.2b)$$

The rf Child law (24) is formally identical to the dc Child law [3b, 4, 5] (replace \bar{U} by U).

The waveform of the rf discharge current determines the value of the numerical factor K .

Now we can translate the rf sheath equations (8) – (11), (14), (16) into normalized form.

$$\frac{v}{v_i} = \frac{\tilde{q}}{\bar{q}} \frac{\varphi_+ - \varphi_-}{2\pi} \quad (9') \quad \frac{d\varepsilon}{dr} = 2 \frac{v}{v_i} \quad (10') \quad \frac{d\eta}{dr} = 2 \frac{\varepsilon}{v_i} \quad (11')$$

$$\frac{d\sigma}{dr} = 2 \frac{1}{v_i} \quad (8') \quad \frac{du}{dr} = -2(\sigma(1) - \sigma) \quad (16')$$

Collisionless ion motion :

$$\frac{1}{v_i} = \sqrt{2\eta} \quad (14'a)$$

Collisional ion motion :

$$\frac{1}{v_i} = \sqrt{\varepsilon} \quad (14'b)$$

V. General rf Sheath Solution

Once we have calculated $\varphi_+(r)$ and $\varphi_-(r)$ for a specific total current $J_t(\varphi)$ from (6), we can go on to solve (8') – (11'), (14'), (16') for $\sigma(r)$, $v_i(r)$, $v(r)$, $\varepsilon(r)$, $\eta(r)$, $u(r)$.

Electric field (r acts as a space-coordinate) :

$$\varepsilon = 2 \frac{\tilde{q}}{\bar{q}} \int_0^r dr \frac{\varphi_+ - \varphi_-}{2\pi} \quad (25)$$

Ion density, net charge carrier density, potential (r acts as a space-coordinate) :

Collisionless rf sheath

$$\frac{1}{v_i} = \frac{\tilde{q}}{\bar{q}} \frac{\varphi_+ - \varphi_-}{2\pi} \frac{1}{v} = 2 \int_0^1 dr \varepsilon \quad (26a)$$

$$\eta = \frac{1}{2} \frac{1}{v_i^2} \quad (27a)$$

Collisional rf sheath

$$\frac{1}{v_i} = \frac{\tilde{q}}{\bar{q}} \frac{\varphi_+ - \varphi_-}{2\pi} \frac{1}{v} = \sqrt{\varepsilon} \quad (26b)$$

$$\eta = 2 \int_0^1 dr \varepsilon^{3/2} \quad (27b)$$

Distance plasma / sheath edge to electron step, sheath voltage (r acts as a time-coordinate) :

Collisionless rf sheath

$$\sigma = 2 \int_0^1 dr \frac{1}{v_i} \quad (28a)$$

$$u = 2 \int_0^1 dr (\sigma(1) - \sigma) \quad (29a)$$

Collisional rf sheath

$$\sigma = 2 \int_0^1 dr \sqrt{\varepsilon} \quad (28b)$$

$$u = 2 \int_0^1 dr (\sigma(1) - \sigma) \quad (29b)$$

$v_i(r)$, $v(r)$, $\varepsilon(r)$, $\eta(r)$ from (25) – (27) and $\sigma(r)$ from (28) determine the spatial dependences of v_i , v , ε , η implicitly. Only when $\sigma(r)$ can be inverted, can we insert $r(\sigma)$ into $v_i(r)$, $v(r)$, $\varepsilon(r)$, $\eta(r)$ and replace σ by ξ (because the time-dependence via r drops out) to obtain the explicit spatial dependences $v_i(\xi)$, $v(\xi)$, $\varepsilon(\xi)$, $\eta(\xi)$. It turns out that the explicit solutions $v_i(\xi)$, $v(\xi)$, $\varepsilon(\xi)$, $\eta(\xi)$ can only be calculated for the square wave total current, but not for the sinusoidal total current.

VI. rf Sheath Solution for the Square Wave Total Current

We calculate $\varphi_+(r)$, $\varphi_-(r)$, $\sigma(r)$, $v_i(r)$, $v(r)$, $\varepsilon(r)$, $\eta(r)$, $u(r)$ for the square wave total current.

The square wave total current can be written as

$$J_t(\varphi) = -|J_t| \text{sign}(\varphi) \quad (30)$$

with $|J_t|$ a constant. The discharge can only be sustained for $|J_t| > J_i$. The sheath will immediately start to charge up, when the total current changes sign from negative to positive, see fig. 2 :

$$\varphi_-(1) = \pi \quad (31.1)$$

The sheath charge amplitude for the square wave current (30) is

$$\tilde{q} = \frac{\pi}{2} \frac{|J_t| - J_i}{\omega} \quad (3.1')$$

From (3.1') and

$$\tilde{q} = \frac{\varphi_+(1)}{2} \frac{|J_t| + J_i}{\omega} \quad (3.2')$$

follows the phase angle $\varphi_+(1)$:

$$\varphi_+(1) = \pi \frac{|J_t| - J_i}{|J_t| + J_i} \quad (31.2)$$

We note that it takes the sheath one half period, $\Delta\varphi = -\varphi_-(1) = \pi$, to charge up, and less than one half period, $\Delta\varphi = \varphi_+(1) < \pi$, to discharge, see fig. 2. The ion current always tends to discharge the sheath.

The time-averaged sheath charge for the square wave current (30) is

$$\bar{q} = \frac{|J_t|}{\omega} \frac{\varphi_+^2(1) + \varphi_-^2(1)}{4\pi} + \frac{J_i}{\omega} \frac{\varphi_+^2(1) - \varphi_-^2(1)}{4\pi} = \frac{\pi}{2} \frac{|J_t|}{\omega} \frac{|J_t| - J_i}{|J_t| + J_i} \quad (4')$$

We combine eq. 3.1', 4' to

$$\frac{\bar{q}}{\tilde{q}} = \frac{1}{1 + J_i/|J_t|} \quad (32.1) \quad \frac{J_i}{|J_t|} = \frac{1 - \bar{q}/\tilde{q}}{\bar{q}/\tilde{q}} \quad (32.2)$$

The phase angles $\varphi_+(r)$ and $\varphi_-(r)$ for the square wave current (30) follow from

$$r = \begin{cases} -\frac{\varphi_-}{\pi} & (6.1') \\ \frac{\varphi_+}{\pi} \frac{|J_t| + J_i}{|J_t| - J_i} = \frac{\varphi_+}{\pi} \frac{1}{2\bar{q}/\tilde{q} - 1} & (6.2') \end{cases} \Rightarrow \frac{\varphi_+ - \varphi_-}{2\pi} = r \frac{\bar{q}}{\tilde{q}}$$

Electric field (r acts as a space-coordinate) :

$$\varepsilon = r^2 \quad (25')$$

$\varepsilon(1) = 1$ follows from the normalization of the electric field, (17) : the electric field unit \bar{q}/ε_0 is the (time-averaged) electric field at the electrode.

Ion density, net charge carrier density, potential (r acts as a space-coordinate) :

Collisionless rf sheath

$$\frac{1}{v_i} = \frac{r}{v} = \frac{2}{3}r^3 \quad (26'a)$$

$$\eta = \frac{2}{9}r^6 \quad (27'a)$$

Collisional rf sheath

$$\frac{1}{v_i} = \frac{r}{v} = r \quad (26'b)$$

$$\eta = \frac{1}{2}r^4 \quad (27'b)$$

Distance plasma / sheath edge to electron step, sheath voltage (r acts as a time-coordinate) :

Collisionless rf sheath

$$\sigma = \frac{1}{3}r^4 \quad (28'a)$$

$$u = \frac{8}{15} - \frac{2}{3}r + \frac{2}{15}r^5 \quad (29'a)$$

Collisional rf sheath

$$\sigma = r^2 \quad (28'b)$$

$$u = \frac{4}{3} - 2r + \frac{2}{3}r^3 \quad (29'b)$$

By inserting (28') in (25') - (27'), η , ε , v and v_i can be related to the distance plasma / sheath edge to electron step, σ . Since the time-dependence (in r) drops out, we replace σ by the distance from the plasma / sheath edge, ξ . (

Collisionless rf sheath

$$\eta = \frac{2}{9}(3\xi)^{3/2} \quad (33a)$$

$$\varepsilon = (3\xi)^{1/2} \quad (34a)$$

$$v = \frac{3}{2}/(3\xi)^{1/2} \quad (35a)$$

$$v_i = \frac{3}{2}/(3\xi)^{3/4} \quad (36a)$$

Collisional rf sheath

$$\eta = \frac{1}{2}\xi^2 \quad (33b)$$

$$\varepsilon = \xi \quad (34b)$$

$$v = 1 \quad (35b)$$

$$v_i = 1/\xi^{1/2} \quad (36b)$$

In the collisionless rf sheath, $\eta(\xi)$, $\varepsilon(\xi)$, $v(\xi)$ and $v_i(\xi)$ follow power laws, with the respective exponents α , $\alpha-1$, $\alpha-2$, and (from **(27a)**) $-\alpha/2$, where $\alpha = 3/2$.

The corresponding power laws for the collisionless dc sheath are obtained for $\alpha = 4/3$ [**3b**, **4**].

In the collisional rf sheath, $\eta(\xi)$, $\varepsilon(\xi)$, $v(\xi)$ and $v_i(\xi)$ follow power laws, with the respective exponents α , $\alpha-1$, $\alpha-2$, and (from **(26b)**) $(1-\alpha)/2$, where $\alpha = 2$.

The corresponding power laws for the collisional dc sheath are obtained for $\alpha = 5/3$ [**5**].

The differences between the power laws for the dc sheath and for the rf sheath are due to the electrons partially screening the ions in the rf sheath.

We note the numerical factor in the Child-law for the rf sheath :

Collisionless rf sheath

$$K = \frac{3}{4} \frac{\tilde{q}}{\bar{q}} \quad (24.2'a)$$

Collisional rf sheath

$$K = 2 \frac{\tilde{q}}{\bar{q}} \quad (24.2'b)$$

For comparison we note the numerical factor in the Child-law for the dc sheath :

Collisionless dc sheath

$$K = 4/9 = 0.44$$

Collisional dc sheath

$$K = \sqrt{2 \times 5^3 / 3^5} = 1.01$$

The numerical factor K depends weakly, via \bar{q}/\tilde{q} , on the ion current J_i . From (32.1) and $0 < J_i < |J_1|$ follows $1 < \tilde{q}/\bar{q} < 2$. K is therefore always larger for the rf sheath than for the dc sheath. The difference is due to the charge screening in the rf sheath.

VII. Comparison of the rf Sheath Solutions

for Sinusoidal and Square Wave Total Current

The rf sheath solution for the sinusoidal total current in [1,2] was obtained assuming a small ion current : $J_i/J_1 \rightarrow 0$ (or $\bar{q}/\tilde{q} = 1$). In this section, the rf sheath solution for the square wave total current is presented for the same limit.

1. Comparison of the spatial dependences of the potential, electric field, net charge carrier density and ion density in the rf sheath, for sinusoidal and square wave total current.

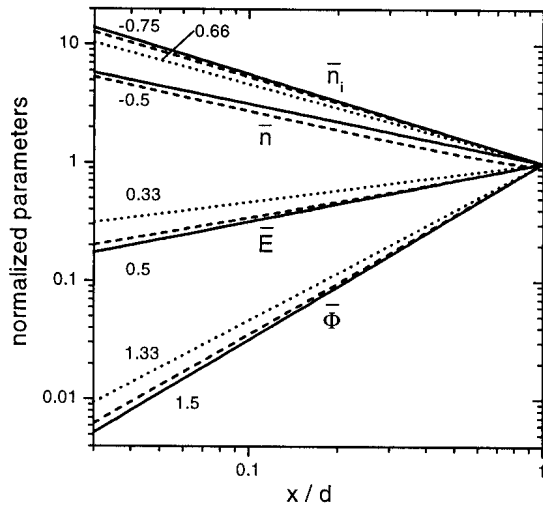


figure 3a : collisionless sheath

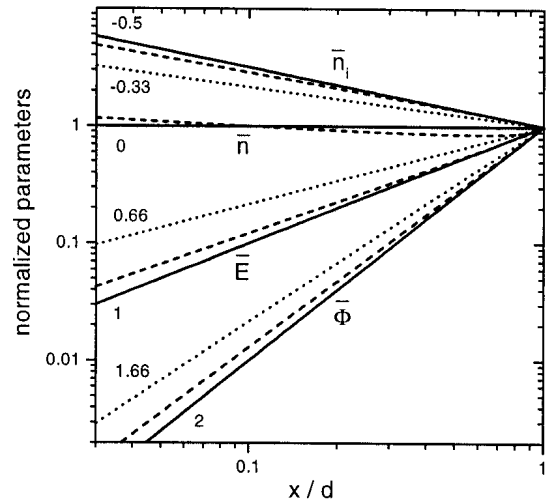


figure 3b : collisional sheath

Potential, electric field, net charge carrier density and ion density in the rf sheath - for square wave total current (solid), and for sinusoidal total current (dashed) - and in the dc sheath (dotted; net charge carrier density = ion density), versus distance from the plasma / sheath edge. All parameters are normalized to their values at the electrode. The exponents in the power laws for the rf sheath (square wave total current) and for the dc sheath are indicated.

In fig. 3 we find :

The spatial dependences of the potential, electric field, net charge carrier density and ion density are similar in the rf sheath and in the dc sheath.

The spatial dependences of the potential, electric field, net charge carrier density and ion density in the rf sheath are almost identical for sinusoidal and square wave total current. The power laws found for the square wave current are therefore also valid to a good approximation for the sinusoidal current.

2. Comparison of the time dependences of the distance electron step to electrode in the rf sheath, and of the rf sheath voltage, for sinusoidal and square wave total current.

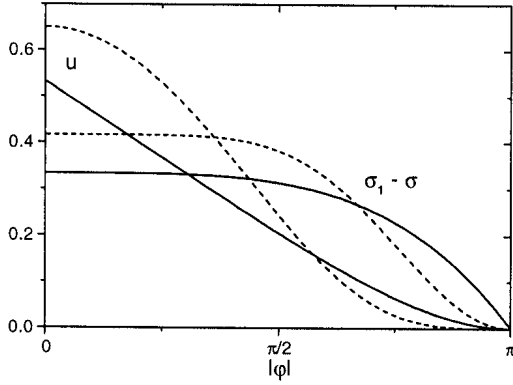


figure 4a : collisionless rf sheath

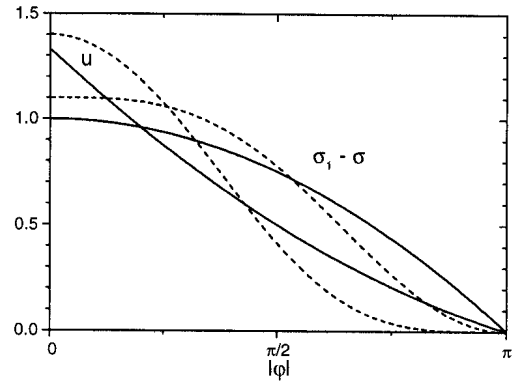


figure 4b : collisional rf sheath

Normalized distance electron step to electrode, and normalized sheath voltage, versus rf phase angle, for square wave total current (solid) and sinusoidal total current (dashed).

In fig. 4 we find :

The time-dependences of the distance electron step to electrode in the rf sheath, and of the rf sheath voltage, are different for sinusoidal and square wave total current : the electron step runs through approximately the same ion distribution in the sheath, with time-dependences imposed by the two current waveforms.

At this point, let us check the form of the voltage across the symmetric rf discharge. The voltage across the bulk plasma is neglected. The two sheath voltages are out of phase by $\Delta\varphi = \pi$, and the discharge voltage is $U(\varphi) - U(\varphi \pm \pi)$. In the limit $J_i/J_t \rightarrow 0$ considered in this section (no power dissipation), the symmetric rf discharge is expected to behave similarly to a capacitance. Therefore, for the square wave total current, we expect a discharge voltage close

to triangular, and for the sinusoidal total current, we expect a discharge voltage close to cosinusoidal. In fig. 5, we find these expectations confirmed.

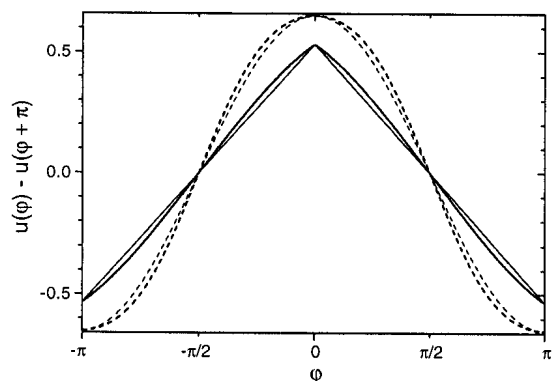


figure 5a : collisionless rf sheath

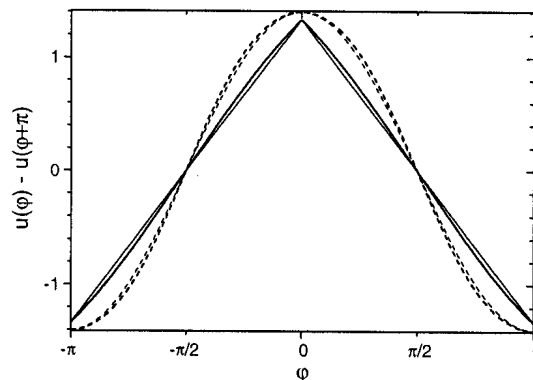


figure 5b : collisional rf sheath

Normalized voltage across the symmetric rf discharge, versus rf phase, for a square wave discharge current (solid line) and a sinusoidal discharge current (dashed). Also shown are the triangular (thin, solid) and cosinusoidal (thin, dashed) discharge voltages (matched to the maximum voltages) expected from the single capacitance equivalent circuit.

3. Comparison of selected rf sheath parameter values, for sinusoidal and square wave total current.

In table 1 we present the selected rf sheath parameter values. For square wave total current, they follow from (24') - (29'); for sinusoidal total current, they are taken from [1,2], and have been corrected for the different normalization, as explained in the Appendix.

	square wave	sinus
σ_1	$1/3 = 0.33$	$5/12 = 0.42$
u_0	$8/15 = 0.53$	$125/192 = 0.65$
$\eta_1 = \bar{u}$	$2/9 = 0.22$	$9/32 = 0.28$
ϵ_1	1	1
$v_1 = v_{i1}$	$3/2 = 1.5$	$4/3 = 1.33$
\bar{u}/u_0	$5/12 = 0.416$	$54/125 = 0.432$
K	$3/4 = 0.75$	$200/243 = 0.82$

table 1a : collisionless rf sheath

	square wave	sinus
σ_1	1	1.10
u_0	$4/3 = 1.33$	1.40
$\eta_1 = \bar{u}$	$1/2 = 0.5$	0.57
ϵ_1	1	1
$v_1 = v_{i1}$	1	1
\bar{u}/u_0	$3/8 = 0.375$	0.405
K	2	2.1

table 1b : collisional rf sheath

Normalized rf sheath parameter values :

sheath width

σ_1

maximum sheath voltage

u_0

time-averaged sheath voltage

\bar{u}

potential at the electrode

η_1

electric field at the electrode

ϵ_1

net charge carrier density at the electrode

v_1

ion density at the electrode

v_{i1}

time-averaged sheath voltage to maximum sheath voltage

\bar{u}/u_0

numerical constant in the Child law

K

The rf sheath parameter values presented in table 1 are similar for sinusoidal and square wave total current. The relative variation is less than $1/4$ for the collisionless rf sheath, and less than $1/8$ for the collisional rf sheath.

VIII. Discussion

For both the dc sheath and the rf sheath, the relation between the sheath voltage U , respectively \bar{U} , and the sheath width d , is described by the same Child law : $U, \bar{U} \propto d^{4/3}$, for the collisionless sheath, and $U, \bar{U} \propto d^{5/3}$, for the collisional sheath. The dependence of the dc sheath potential Φ on the the distance from the plasma / sheath edge, x , is obtained by replacing, in the dc Child law, d by x , and U by $-\Phi$. The rf sheath analysis for square wave discharge current now shows, that the analogous substitution in the rf Child law, $d \rightarrow x, \bar{U} \rightarrow -\bar{\Phi}$, is *not* correct : due to the partial charge screening in the rf sheath, the spatial dependence of the sheath potential becomes $-\bar{\Phi} \propto x^{3/2}$ for the collisionless rf sheath, and $-\bar{\Phi} \propto x^2$ for the collisional rf sheath.

Wild and Koidl [6, 7], and Fivaz et al [8], experimentally determined sheath potential power laws $-\bar{\Phi} \propto x^\alpha$ for capacitive rf discharges in Ar, by measuring peak features in the energy distributions of extracted Ar^+ ions. For $P = 0.3 - 3 \text{ Pa}$, $f = 13.56 \text{ MHz}$, $\bar{U} \approx 500 \text{ V}$, $d/\lambda_i \cong 0.5 - 2$ (calculated for $\sigma \cong 45 \text{ \AA}^2$), Wild and Koidl found $\alpha \cong 1.6$ in [6], and $\alpha \cong 1.5$ in [7]. For $f = 13.56 - 42 \text{ MHz}$, $P = 13 \text{ Pa}$, $\bar{U} \approx 60 \text{ V}$, $d/\lambda_i \cong 4 - 8$ (calculated for $\sigma \cong 55 \text{ \AA}^2$), Fivaz et al [8] found $\alpha \cong 2$.

The quoted experiments do not allow to distinguish between the power range, $4/3 < \alpha < 5/3$, naively deduced from the Child law, and $3/2 < \alpha < 2$, found in this report.

Furthermore, the assumptions (A4) – (A7) for our model rf sheath are seldom well justified for real discharges, and may impair the agreement between the present theory and experiment.

IX. Conclusion

Lieberman's analysis of the high voltage, capacitive rf sheath, both for collisionless [1] and for collisional [2] ion motion, is carried out for the square wave rf discharge current.

The rf sheath solutions for the square wave current, in this report, and for the sinusoidal current, in refs. [1,2], are compared.

For the square wave discharge current, the time-averaged sheath potential, electric field, net charge carrier density, and the ion density are found to be related to the distance from the plasma / sheath edge by power laws.

For the collisionless rf sheath, the respective exponents are $3/2$, $1/2$, $-1/2$, and $-3/4$ (compared to $4/3$, $1/3$, $-2/3$, $-2/3$ for the collisionless dc sheath).

For the collisional rf sheath, the respective exponents are 2, 1, 0, and $-1/2$ (compared to $5/3$, $2/3$, $-1/3$, $-1/3$ for the collisional dc sheath).

These power laws are found to be valid to a good approximation also for the sinusoidal discharge current. For fixed sheath charge amplitude and ion current, the values of rf sheath parameters such as the sheath width, and the time-averaged sheath voltage, are found to be similar for sinusoidal and for square wave discharge current. The 'time-averaged rf sheath' seems to be robust with respect to change of the discharge current waveform.

Appendix

In refs. [1,2], Lieberman normalizes the sheath parameters by means of the unit of voltage : electron temperature T_e , the unit of the number density : bulk plasma ion density n_{i0} , and the three units of length : Debye-length $\lambda_D = (\epsilon_0 T_e / n_{i0} e)^{1/2}$, amplitude of the matrix - sheath width $\tilde{s}_M = \tilde{q} / en_{i0}$ (the ion density in the matrix sheath is constant; $2\tilde{s}_M$ is the matrix sheath width), and, for the collisional rf sheath, ion mean free path λ_i (to which we keep associated the factor $2/\pi$).

In the normalization equations (17) – (23), we set $\bar{q} = \tilde{q}$ (Lieberman assumed $J_i \ll J_0$), replace the ion current J_i by $en_{i0}(eT_e/m_i)^{1/2}$ (Bohm criterion), simplify the resulting expressions with λ_D and \tilde{s}_M , and obtain :

$$\epsilon \times \frac{\tilde{s}_M^2 T_e}{\lambda_D^2 \tilde{s}_M} = \bar{E} \quad (17')$$

Collisionless rf sheath

$$\left. \begin{array}{l} \xi \\ \sigma \end{array} \right\} \times \frac{\tilde{s}_M^2}{\lambda_D^2} \tilde{s}_M = \left\{ \begin{array}{l} x \\ s \end{array} \right. \quad (18'a)$$

$$(19'a)$$

$$\left. \begin{array}{l} v \\ v_i \end{array} \right\} \times \frac{\lambda_D^2}{\tilde{s}_M^2} n_{i0} = \left\{ \begin{array}{l} \bar{n} \\ n_i \end{array} \right. \quad (20'a)$$

$$(21'a)$$

$$\left. \begin{array}{l} \eta \\ u \end{array} \right\} \times \frac{\tilde{s}_M^4}{\lambda_D^4} T_e = \left\{ \begin{array}{l} -\bar{\Phi} \\ U \end{array} \right. \quad (22'a)$$

$$(23'a)$$

Collisional rf sheath

$$\left. \begin{array}{l} \xi \\ \sigma \end{array} \right\} \times \frac{\sqrt{\frac{2}{\pi}} \lambda_i \tilde{s}_M}{\lambda_D} \tilde{s}_M = \left\{ \begin{array}{l} x \\ s \end{array} \right. \quad (18'b)$$

$$(19'b)$$

$$\left. \begin{array}{l} v \\ v_i \end{array} \right\} \times \frac{\lambda_D}{\sqrt{\frac{2}{\pi}} \lambda_i \tilde{s}_M} n_{i0} = \left\{ \begin{array}{l} \bar{n} \\ n_i \end{array} \right. \quad (20'b)$$

$$(21'b)$$

$$\left. \begin{array}{l} \eta \\ u \end{array} \right\} \times \frac{\tilde{s}_M^2 \sqrt{\frac{2}{\pi}} \lambda_i \tilde{s}_M}{\lambda_D^3} T_e = \left\{ \begin{array}{l} -\bar{\Phi} \\ U \end{array} \right. \quad (22'b)$$

$$(23'b)$$

Lieberman defined a parameter H , which is a combination of the three units of length :

$$\pi H = \tilde{s}_M^2 / \lambda_D^2 \quad (\text{collisionless rf sheath}), \text{ and } \pi^{1/2} H = \left(\frac{2}{\pi} \lambda_1 \tilde{s}_M \right)^{1/2} / \lambda_D \quad (\text{collisional rf sheath}).$$

He normalized the sheath parameters with H . Our normalization differs from Lieberman's normalization by the prefactor π (collisionless rf sheath), and $\pi^{1/2}$ (collisional rf sheath).

Acknowledgements :

The authors thank Dr. Laurent Sansonnens for suggestions to improve the manuscript.

1. M. A. Lieberman, IEEE Trans. Plasma Sci. **16**, 638 (1988)
2. M. A. Lieberman, IEEE Trans. Plasma Sci. **17**, 338 (1989)
3. M. A. Lieberman, A. J. Lichtenberg, Principles of Plasma Discharges and Material Processing, John Wiley & Sons, New York, 1994 (a : p. 137; b : p. 165)
4. B. Chapman, Glow Discharge Processes, John Wiley & Sons, New York, 1980 (p. 107)
5. R. Warren, Phys. Rev. **98**, 1658 (1955)
6. C. Wild, P. Koidl, Appl. Phys. Lett. **54**, 505 (1989)
7. C. Wild, P. Koidl, J. Appl. Phys. **69**, 2909 (1991)
8. M. Fivaz, S. Brunner, W. Schwarzenbach, A. A. Howling & Ch. Hollenstein, Plasma Sources Sci. Technol. **4**, 373 (1995)